Catalysis Science & Technology

Accepted Manuscript

This article can be cited before page numbers have been issued, to do this please use: M. Wolfsgruber, P. Patil, C. M. Pichler, R. H. Bischof, S. Budnyk, C. Paulik, B. V.M. Rodrigues and A. Slabon, *Catal. Sci. Technol.*, 2023, DOI: 10.1039/D3CY00897E.

ROYAL SOCIETY OF CHEMISTRY

rsc.li/catalysis

View Article Online
DOI: 10.1039/D3CY00897E

ARTICLE

Potential Dependence of Gluconic Acid to Glucose Electroreduction on Silver

Received 00th January 20xx,
Accepted 00th January 20xx

DOI: 10.1039/x0xx00000x

Maria Wolfsgruber,*[a] Prathamesh Patil,[b] Christian M. Pichler,[b,c] Robert H. Bischof,[d] Serhiy Budnyk,[e] Christian Paulik,[f] Bruno V. M. Rodrigues,*[g] and Adam Slabon*[g]

The electrocatalytic conversion of gluconic acid, an aldonic acid, as a model component of the spent sulfite liquor (SSL) represents a green approach for side-stream valorization. The biotechnological valorization of the SSL to more valuable products is inhibited by aldonic acids. Here, we discovered silver as electrocatalyst for the reduction of gluconic acid to glucose as a sustainable strategy to convert aldonic acids into fermentable carbohydrates. A potential screening in a two-electrode compartment cell was investigated and showed the best conversion at −1.56 V *vs*. reversed hydrogen electrode (RHE) with 0.296 mmol·L^{-1}. The conversion rate decreased with higher and lower potentials than −1.56 V *vs.* RHE. SEM, EDS, and XPS analyses revealed no clear influence of the reaction on the electrocatalyst. LEIS measurements indicated only ion adsorption from the electrolyte and a slight surface oxidation. The electrocatalytic behavior of silver reveals a similar trend as for the electrocatalytic CO_2 reduction reaction and nitrogen reduction reaction, where a maximum conversion is reached at one cathodic potential before the hydrogen reduction reaction becomes dominant. This highlights a key challenge in merging electrocatalysis and the biorefinery concept to create a bioelectrofinery for side-stream valorization, a crucial element of a bio-circular-green economy.

Introduction

In terms of economic, ecological, and social aspects, sustainable processes are the main pillars for future industries to ensure the achievement of the global climate targets. In this context, it is important to optimize processes, valorize side-streams and resort to renewable raw materials instead of fossil resources. [1,2] Biorefineries are an opportunity to expand the capacity of renewable and sustainable processes while simultaneously enabling the reduction of petroleum-based materials and chemicals. [2–4] As renewable energies have become economically marketable and established, e.g., power and solar energy, the combination of biorefineries in connection with green energy appears as a sustainable solution for the production of platform chemicals. [5,6] In 2022, the global biorefinery market price was USD 141.88 billion. The biorefinery market is fast increasing with a compound annual growth rate (CAGR) forecast of 8.2% by 2027 and a global biorefinery market price projected to be USD 210.3 billion in 2027. [7] Biomass is rich in various carbon sources, which can be processed to platform chemicals and precursors. [3] The biomass in the biosphere is approximately 550 gigatons of carbon (Gt C), where the biggest part with approximately 450 Gt C is located in the plant sector.[8] In this context, spent sulfite liquor (SSL) is an abundantly available side-stream in the pulp and paper industry. SSL is formed during the sulfite pulping process and consists of various wood degradation products, with lignosulfonates, soluble carbohydrates and aldonic acids being its main constituents.

An undesired consequence of the sulfite pulp process is the partial formation of glucose monomers from cellulose and hemicelluloses, which can further react to produce gluconic acid in an oxidative environment. This reaction is not limited to glucose alone; all aldoses generated during the process undergo partial oxidation, resulting in the formation of aldonic acids. [9,10] However, the presence of aldonic acids poses inhibitory effects on the efficient fermentation of SSL in biorefineries. [11] Furthermore, the separation of aldonic acids from aldoses is challenging due to their similar size, structure, and properties. [10,12]

To facilitate the processing of SSL, it is preferable to convert aldonic acids into fermentable substances. One prospective approach for SSL valorization involves the reduction of gluconic acid to glucose. The global market price of glucose was USD 42.9 billion in 2020, with a predicted compound

[a] Kompetenzzentrum Holz GmbH, Altenberger Straße 69, 4040 Linz, Austria
[b] Centre for Electrochemistry and Surface Technology, TFZ – Wiener Neustadt, Viktor-Kaplan-Strasse 2, 2700 Wr. Neustadt, Austria
[c] Institute of Applied Physics, Vienna University of Technology, Wiedner Hauptstr. 8-10/134, 1040 Wien, Austria
[d] Lenzing AG, Werkstraße 2, 4860 Lenzing, Austria
[e] AC2T Research GmbH, Viktor Kaplan-Straße 2/c, 2700 Wiener Neustadt, Austria
[f] Institute for Chemical Technology of Organic Materials, Johannes Kepler University Linz, Altenberger Straße 69, 4040 Linz, Austria
[g] Chair of Inorganic Chemistry, University of Wuppertal, Gaußstraße 20, 42119 Wuppertal, Germany, E-mail: slabon@uni-wuppertal.de, manzolli@uni-wuppertal.de

† Electronic Supplementary Information (ESI) available: [details of any supplementary information available should be included here]. See DOI: 10.1039/x0xx00000x

annual growth rate (CAGR) of 5.0% from 2020 to 2028. [13] The conversion to glucose not only enables fermentation but also serves as a precursor for the production of more valuable products, such as sorbitol. [14] Historically, the conversion of gluconic acid into glucose was reported in 1927 by Glattfeld et al. using classical hydrothermal conversion with platinum black as a catalyst. Although the process achieved a conversion rate of 14-28%, it could not be successfully replicated for other aldonic acids. [15] However, the use of high temperatures and pressures in thermal hydrogenation renders it unsustainable and undesirable due to its environmental impacts and safety concerns. Additionally, challenges such as catalyst recovery, ageing, and poisoning hinder the feasibility of a sustainable process. [6,16]

Within the context of the SSL, the presence of sulfur components has been observed to function as catalyst poisons, impeding hydrogenation reactions. [10,17] Moreover, in the selective hydrothermal reduction of glucose to sorbitol using Raney nickel as a catalyst, gluconic acid also serves as a catalyst poison. [18] Another drawback lies in the challenge of achieving selective thermal hydrogenation, as it exhibits low selectivity. Consequently, not only gluconic acid but also other diverse components would undergo hydrogenation in the SSL. [19,20]

A more ambitious and better approach is the use of electrocatalytic processes, which combine renewable and green energies with sustainable raw materials. [3,6] Extensive research has been conducted on electrochemical synthesis to valorize various biomass substances and side-streams in the pulp and paper industry. [1] For instance, Liu et al. investigated the electrochemical oxidation of glucose to gluconic acid, followed by its further oxidation to glucaric acid. [20] Governo et al. reported on the electrochemical oxidation of xylose to xylonic acid and shorter oxidation products like glyoxylic acid. [21] The electrochemical reduction of furfural to furfuryl alcohol in a microchannel flow reactor was elaborated by Cao et al. [22] Furthermore, the oxidation of furfural to furoic acid was carried out electrochemically by Parpot et al. [23]

The electrocatalytic reduction of gluconic acid and xylonic acid to glucose and xylose, respectively, was reported on a previous investigation of our group. [24] At a potential of −1.04 V *vs.* reversed hydrogen electrode (RHE), using gold as the active electrocatalytic material, a conversion of 0.43% of gluconic acid to glucose could be achieved in the H-cell. [24] Gold is known to be one of the most expensive metals (USD 1964 per ounce in June 2023), whereas silver, in comparison, is approximately 100 times cheaper (USD 23.89 per ounce in June 2023). [25,26] The cost difference is one of the reasons why silver was considered as an alternative electrode material in this study, making it a more economically viable while also a benign approach. [25,26] However, it is not just the economic factor that favors silver as an electrocatalytic material; the ecological impact also supports its preference. [27] The Life Cycle Assessment analysis reveals that gold has a greater impact on global warming, higher cumulative energy demand, increased freshwater eutrophication, and greater toxicity to humans compared to silver. In general, gold exhibits a higher global warming potential and poses a greater risk to ecosystem and health. [27] Silver as electrocatalytic material is already used for the reduction of carbon dioxide to carbon monoxide, hydrogen, formate, methane, methanol, and ethanol.[28] Several electrolytic applications for silver are known, such as silver-based gas-diffusion electrodes for the chloralkali electrolysis [29] or the 5-(hydroxymethyl)furfural to 2,5-bis(hydroxymethyl)furan reaction on an oxide-derived silver working electrode, which can be further used for polyesters and polyurethan foams.[30]

The use of electrocatalysis in biorefineries remains an underexplored field, despite its high potential for biomass and side-stream valorization following the principles of *Green Chemistry*. To date, only our previous study has addressed the electrocatalytic reduction of aldonic acids to the corresponding biomass sugars. [24] In this investigation, we tested different commercially available electrocatalytic materials and present a more sustainable approach by using silver as electrocatalyst for the reduction of gluconic acid to glucose within a green framework (Scheme 1).

View Article Online
DOI: 10.1039/D3CY00897E

ARTICLE

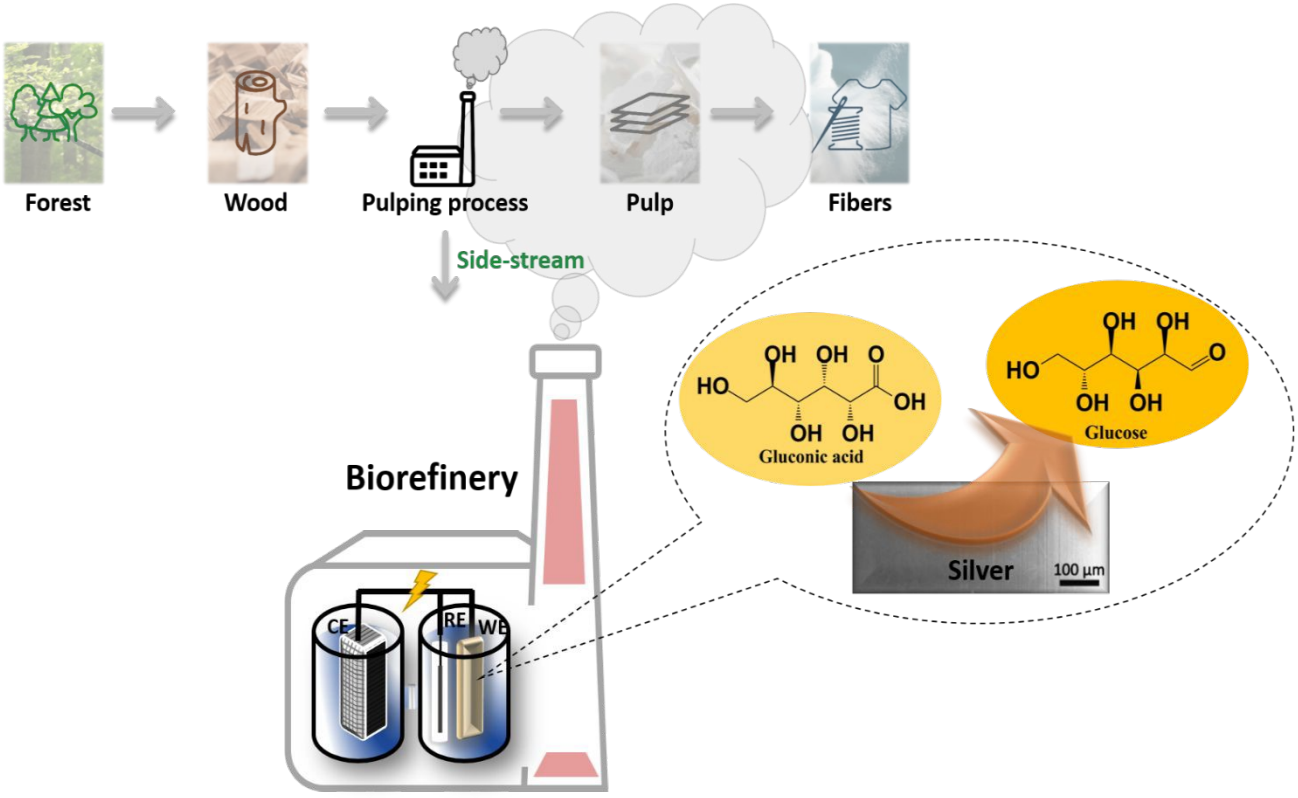

Scheme 1 Schematic illustration of the electrochemical reduction of gluconic acid to glucose in a membrane cell with a 3-electrode setup (CE: counter electrode, WE: working electrode, RE: reference electrode) in an aqueous electrolyte system. The system could be embedded in a pulping process, where a side-stream could be used for the conversion in a biorefinery plant. The electrocatalytic active material is silver and the conversion efficiency is highly dependent on the applied potential.

Experimental

Materials

D-gluconic acid (50%) and the platinum mesh (52 mesh woven from 0.1 mm dia wire, 99.9%, 5x5 cm^2) were purchased from Alfa Aesar and the silver wire (1.0 mm, 99.9%) from abcr GmbH. The tin wire (1.0 mm, 99.998%) was purchased from thermo scentific. The fumapem F-10100 cation exchange membrane was acquired from Fumatech BWT GmbH. Sulfuric acid (H_2SO_4, 95%), sodium hydroxide (NaOH) and nitric acid (HNO_3, 65%) were purchased from VWR and Magnesium sulfate ($MgSO_4$) from Mallinckrodt. In all experiments, DI water and Milli-Q water were used.

Solutions

Gluconic acid (2.5 g) was dissolved in Milli-Q water. 1.5 g of $MgSO_4$ as electrolyte were dissolved separately in Milli-Q water. The two solutions were combined and filled up to a total amount of 100 g with Milli-Q water. The solution was adjusted to a pH of 2.5 with NaOH solution (gluconic acid solution). An electrolyte solution with 1.5 wt% of $MgSO_4$ was used for the second chamber of the membrane cell experiments. Therefore, 1.5 g of $MgSO_4$ were dissolved in 98.5 g Milli-Q water. The solution was adjusted to a pH of 2.5 with H_2SO_4 (electrolyte solution).

Electrocatalysis

The electrochemical reactions were performed in a membrane cell (H-cell) using a 3-electrode setup. A silver wire with a geometric surface area of 3.5 cm^2 was used as working electrode (WE). Prior the reaction the silver wire was polished and rinsed with Milli-Q water. A platinum mesh acted as counter electrode (CE) and an Ag/AgCl (saturated KCl) as reference electrode (RE), respectively. For cleaning, the

platinum mesh was pre-treated with nitric acid and rinsed with Milli-Q water. For the reaction, 50 g of the gluconic acid solution were used in the cathodic chamber of the H-cell and 50 g of the electrolyte solution in the anodic chamber. The reactions were performed at −0.66, −0.86, −1.06, −1.16, −1.26, −1.36, −1.46, −1.56 and −1.66 V *vs.* RHE. The reaction time was up to 8 h. A second experiment was done under the same conditions, but with Sn as WE at −1.16 V *vs.* RHE. As third electrocatalytic material, Pt was tested as WE with the same setup and the same conditions, but at a potential of −1.16 V *vs.* RHE. The calculations of the produced glucose were done accordingly to our previous study. [24]

High performance liquid chromatography (HPLC)

The quantification of gluconic acid and glucose was performed by ion exchange chromatography. As apparatus a Thermo Scientifix ICS 5000+ HPLC system with a Dionex CarboPac SA10 4 × 50 mm pre-column and a Dionex CarboPac SA10 4 × 250 mm separation column was used. For the glucose quantification, DI water and 0.35 M sodium hydroxide solution performed as gradient elution at a flow rate of 1 mL·min^{-1}. The injection volume was 10 μL. The same apparatus was used for the gluconic acid quantification. However, the injection volume was increased to 25 μL and the eluent was a 0.6 M sodium hydroxide solution.

Scanning Electron Microscopy (SEM)

The morphology of the WEs were analyzed using a Thermo Fisher Quanta 450 using an accelerating voltage of 10 kV for the SEM micrographs. The energy-dispersive (EDS) measurements were done by a Phenom pro XL at an accelerating voltage of 15 kV to determine the topography.

X-ray Photoelectron spectroscopy (XPS)

The surface analysis of the silver WE via x-ray photoelectron spectroscopy was determined via a Theta Probe (Thermo Fisher Scientific). The X-ray source was a monochromatic Al Kα one at 1386.6 eV. For metallic silver, the spectrometer was calibrated to 368.21 eV binding energy (BE) of Ag $3d_{5/2}$. Sputtering was performed via an EX05 ion gun with argon cations at 3 keV, 1 μA and 4 mm^2. A base pressure below $5 \cdot 10^{-8}$ Pa was used in the analytic chamber. The X-ray spot lateral resolution was defined as 400 μm. 50 eV BE were used as pass energy for the recording of the detailed spectra. The pass energy of the survey spectra was 200 eV BE. The 2012 NIST XPS database was used as reference for the analyzation of the detected binding states of silver.

Low Energy Ion Scattering spectroscopy (LEIS)

The low energy ion scattering spectroscopy measurements of the silver WE were performed using $^4He^+$ ions accelerated at 3 keV as primary ions. The primary ion beam was incident at an angle normal to the sample surface over an area of 250x250 µm. Ions scattered at an angle of 145° were collected and integrated over the azimuth to generate the spectra. The only surface treatment done was for fresh the silver WE. A thin contamination layer was cleaned with 1 keV Ar for 5 seconds. The sample was assumed to be clean when spectra were consistent with further sputtering. A second measurement of the used silver WE was performed with $^{20}Ne^+$ accelerated at 5 keV to better resolve surface species.

Results and discussion

The linear sweep voltammetry (LSV) curve for the experiment in a two-compartment cell with a gluconic acid concentration of 2.5 wt% and a $MgSO_4$ concentration of 1.5 wt% as electrolyte (named Gluconic acid) is depicted in Figure 1. The second LSV curve was recorded only with the electrolyte solution (1.5 wt% $MgSO_4$, named Electrolyte). Ag wire was used as the WE, a Pt mesh as a CE and an Ag/AgCl (saturated KCl) as a RE. The cathodic current density in the experiment without the gluconic acid was due to the hydrogen evolution reaction (HER). The onset potential for the HER in the electrolyte solution was at approximately −0.7 V *vs*. RHE. For the LSV curve with gluconic acid presented in the solution, the onset potential was at −0.2 V *vs*. RHE. At a potential of −0.7 V *vs*. RHE, we observed a local minimum of the curve, therefore, electrocatalytic experiments were also tested at this potential. A local maximum was observed at a potential of −1.0 V *vs*. RHE. From this potential into the more cathodic region, there was a sharp increase in the cathodic current density. The slope of the curve at this area was very similar to the curve only with the electrolyte solution. In the subsequent experiments, the conversion showed a significant increase starting from −0.86 V *vs*. RHE, reaching its maximum at −1.56 V *vs*. RHE and, then decreasing again. The LSV curves suggest that, starting from −0.86 V *vs*. RHE, both HER and gluconic acid reduction are competitively present.

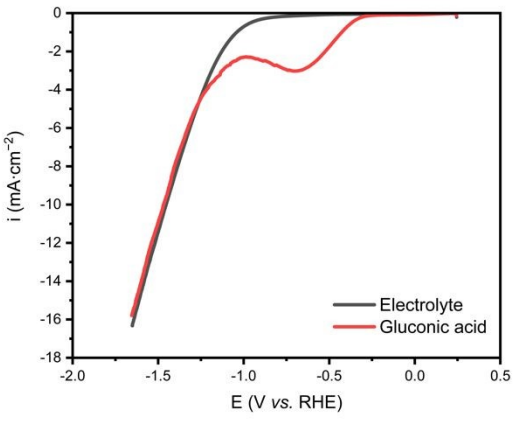

Figure 1 LSV curves of 2.5 wt% gluconic acid and 1.5 wt% $MgSO_4$ (named Gluconic acid) and only 1.5 wt% $MgSO_4$ (named Electrolyte) solutions in the H-cell. As a setup, silver, platinum, and Ag/AgCl (saturated KCl) were used as WE, CE and RE, respectively. The scan rate was 10 mV·s^{-1}.

View Article Online
DOI: 10.1039/D3CY00897E

The chronoamperometry (CA) curves for the experiments with a concentration of 2.5 wt% gluconic acid and an electrolyte concentration of 1.5 wt% in the membrane cell are illustrated in Figure S1. The geometric area of the Ag WE was 3.5 cm^2 and a reaction time of 8 h was considered for all experiments. The potentials used were −0.66, −0.86, −1.06, −1.16, −1.26, −1.36, −1.46, −1.56 and −1.66 V *vs.* RHE. Duplicates of each experiment were performed. Starting from −0.66 to −0.86 V *vs.* RHE, the current became more cathodic. Nevertheless, the current got less cathodic over the reaction time of 8 h for all considered potentials.

The conversion of gluconic acid to glucose could be observed during all reactions. In Table S1, the conversion rates of the gluconic acid, the initial concentrations of gluconic acid and glucose and the concentrations after 4 and 8 h, with corresponding potentials, are listed.

Figure 2 shows the average values of the produced glucose versus the different reaction potentials of the duplicate experiments. The two values for each potential differed less than 20% and for the highest turnover rate, a difference of less than 5% was achieved.

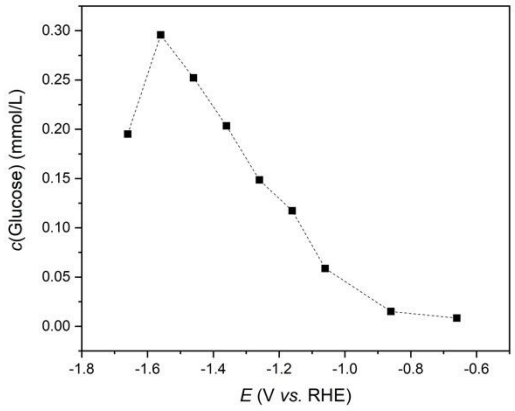

Figure 2 The curve shows the average values of the produced glucose concentration at different potentials. The reactions were performed in a 2.5 wt% gluconic acid solution with an electrolyte ($MgSO_4$) concentration of 1.5 wt% in an H-cell with a reaction time of 8 h. The Ag WE had a geometric surface area of 3.5 cm^2. The reaction potentials were −0.66, −0.86, −1.06, −1.16, −1.26, −1.36, −1.46, −1.56 and −1.66 V vs. RHE.

The highest amount of glucose (0.296 mmol·L^{-1}) was achieved at −1.56 V *vs*. RHE (Figure 2). The curve representing the concentration of produced glucose as a function of the potential exhibits a distribution similar to a Gaussian bell curve, with the peak concentration occurring near the maximum. [24] With higher and lower potentials, a decrease in conversion takes place. The conversion rate increased by two-fold from a reaction potential of −1.26 V *vs.* RHE to −1.56 V *vs*. RHE. The conversation rate further increased by 10-fold when the potential raised from −0.86 V *vs.* RHE to −1.26 V *vs.* RHE. At a potential of −0.66 V *vs.* RHE, the conversion was at its lowest, with only a marginal amount of 0.008 mmol·L^{-1} of gluconic acid being converted to glucose. The observed curve shape can be attributed to the dominance of HER in the more cathodic region. In the less cathodic region, the potential was not sufficient to overcome the activation energy required for the reduction reaction of gluconic acid to glucose. A similar behavior was observed in the CO_2 reduction reaction. [31]

The conversion rates remained consistently below 0.3%. In this case, the conversion rate was limited by the constraints of the setup, preventing an increase in the conversion rate. Due to the resistance and area of the membrane in the H-cell, increasing the electrode surface area is not possible due to the overpotential of the potentiostat.

During the reactions, the conversion of gluconic acid into glucose increased almost linearly at potentials −1.26, −1.16 and −1.06 V *vs.* RHE (Figure 3). Therefore, it can be assumed that there is no inhibition of the reaction over this period. This is in line with our previous study [24], where the inhibition of the reaction by the Pt CE could be excluded. To further prove this, a reaction was carried out with carbon paper as a CE in the same reaction system. [24] For the less cathodic reaction conditions, at −0.66 and −0.86 V *vs.* RHE, only a slightly increase of the conversion of gluconic acid to glucose could be observed. At −0.66 V *vs.* RHE 0.008 mmol·L^{-1} glucose were produced and at −0.86 V *vs.* RHE 0.015 mmol·L^{-1}, respectively. This behavior was also noted under more cathodic conditions at −1.66 V *vs.* RHE, where the glucose concentration increased over a reaction time of 4 h, but then stagnated. At the potentials of −1.56, −1.46 and −1.36 V *vs.* RHE the amount of glucose produced increased non-linearly over a reaction time of 8 h. The highest conversion was achieved in the first hours. Over the whole reaction time, the highest conversion was observed at a potential of −1.56 V *vs.* RHE.

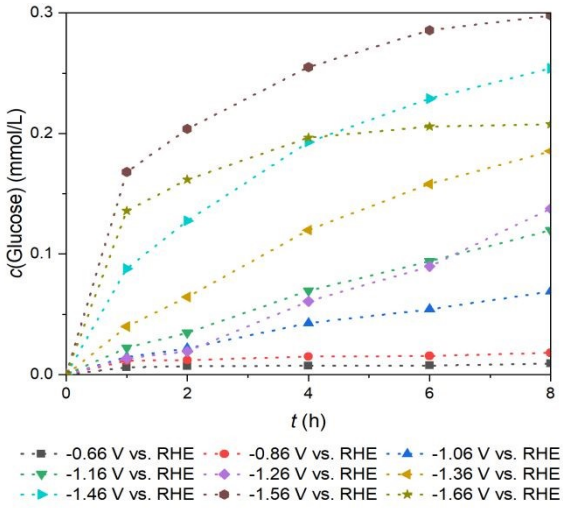

Figure 3 The diagram shows the glucose concentrations versus the reaction times at different potentials. Glucose concentration from the experiments in the H-cell with a 3.5 cm^2 Ag WE. The reactions were performed in a 2.5 wt% gluconic acid solution with an $MgSO_4$ concentration of 1.5 wt%. The different reaction potentials were −0.66, −0.86, −1.06, −1.16, −1.26, −1.36, −1.46, −1.56 and −1.66 V vs. RHE. The reaction time was up to 8 h.

The Faraday efficiencies (FEs) of the conversion of gluconic acid to glucose were calculated in line with the timeline experiments after 1, 2, 4, 6, and 8 h (Table S1). The FEs were calculated based on Equation S1. For all potentials, the highest

View Article Online
DOI: 10.1039/D3CY00897E

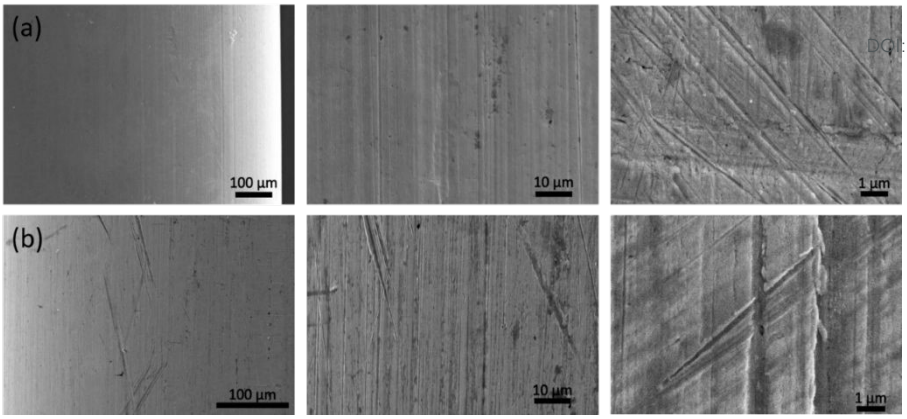

Figure 4 SEM micrographs of the Ag WE with a geometrical surface area of 3.5 cm². (a) Ag wire before the reaction and (b) Ag wire pre-treated by polishing and after the reaction with 1.5 wt% gluconic acid solution with an electrolyte ($MgSO_4$) concentration of 1.5 wt%. The reaction was performed using a 3-electrode setup with a platinum mesh as CE and an Ag/AgCl (saturated KCl) as RE. The reaction time was 8 h and the applied potential −1.56 V vs. RHE in the H-cell.

FE was achieved after 1 h. At the potentials of −0.66, −0.86, −1.36, −1.46, −1.56 and −1.66 V *vs.* RHE, a non-linear decrease was observed over the reaction time (Figure S2). The maximum after 1 h and the subsequent decreases of the FE could indicate the setting of an equilibrium, whereby competing reactions (e.g., HER) may be preferred. At potentials of −1.06, −1.16 and −1.26 V *vs.* RHE the FE was nearly constant. Over the reaction time of 8 h the highest FE was achieved at −1.56 V *vs.* RHE. However, all calculated FEs were below 1% at all potentials for 8 h reactions. The curve shape of the produced glucose concentration over the reaction time is in line with the FEs. With the decreasing FEs over the reaction time, a flattening of the curves of the glucose concentrations was observed.

For comparison of the Ag WE with the previously reported Au WE [24], the glucose concentration of a reaction with a 3.5 cm² Au WE in an H-cell was determined. The reaction potential and reaction time were the one previously stablished (−1.06 V *vs.* RHE and 8 h). The reaction substrate was a 2.5 wt% gluconic acid solution with a 1.5 wt% $MgSO_4$ concentration as electrolyte. The produced glucose concentration was 0.77 mmol·L^{-1} and the conversion rate 0.61%. The conversion using the Au WE was more than 2.5 times higher than with the Ag WE.

Despite the higher turnover with the Au electrode, Ag is a preferred material due to its lower price (approximately 100 times cheaper than Au). [32] Furthermore, it is worth noting that silver is approximately 15 to 20 times more abundant in the Earth's crust. [33]

To test other commercially available electrocatalytic materials, similar reactions of gluconic acid to glucose with tin (Sn) and platinum (Pt) as WEs were done. The detailed experimental conditions can be found in the supporting information (IV. Experiments). Only a small conversion of gluconic acid to glucose could be detected for tin (0.02 mmol·L^{-1} glucose) and platinum (0.03 mmol·L^{-1} glucose) as electrocatalysts, after 8 h. In comparison to Sn, the produced amount of glucose was approximately 15 times higher with Ag as WE. These results

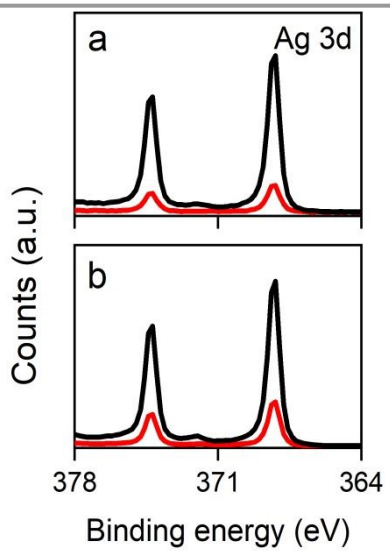

Figure 5 XPS patterns of Ag 3d of the Ag WE with a geometric surface area of 3.5 cm². XPS patterns of Ag 3d (a) before and (b) after the reaction in a 2.5 wt% gluconic acid solution with a $MgSO_4$ concentration of 1.5 wt%. The reaction was performed in an H-cell. The black line indicates the measurements with sputtering and the red line without sputtering.

are in contrast with previously published work from electrochemical CO_2 reduction, in which Sn is handled as a very active and promising electrocatalyst. [34] By comparing Pt and Ag as WEs, the conversion on Ag was approximately 9 times higher than with Pt. Ag is therefore also preferred as electrocatalytic material against Sn and Pt.

Scanning electron microscopy (SEM) micrographs of the Ag WE before the reaction (Figure 4a) and pre-treated by polishing and after the reaction (Figure 4b) are presented. The micrographs showed a difference in the surface structure of the polished WE after use. Slightly more scratches were visible on the surface from the polished one. The purpose of the polishing was to remove any deposits or oxidation products that may have formed on the surface due to the surrounding environment.

No significant differences between the two wires (before and after the reaction) could be detected by energy-dispersive X-ray spectroscopy (EDS). The EDS measurements showed that, even after the reaction, the topography of the wire still consists of over 95 wt% pure silver and traces of oxygen and carbon. No influence of the reaction on the surface of the wire could be detected.

X-ray photoelectron spectroscopy (XPS) measurements with and without sputtering of the Ag WE surface were performed before and after the reaction (Figure 5). The two spin-orbit coupling components $3d_{5/2}$ at 368.2 eV and $3d_{3/2}$ at 474.2 eV of Ag 3d were visible during the XPS analysis. No significant shifts between the XPS patterns could be detected; therefore, the electrode surface was not measurably affected by the reactions.

Low Energy Ion Scattering spectroscopy (LEIS) measurements were performed on the Ag WE before and after the reaction (Figure 6). By comparing the spectra, we can see the presence of additional peaks for the post-reaction WE. These peaks correspond to the presence of O, S, Mg and other species that could have originated from the electrolyte. This suggests the possibility of adsorption of SO_4^{2-} and Mg^{2+} ions on the surface of the Ag electrode, along with surface oxidation of Ag itself. The components of the electrolyte are likely adsorbed onto the surface of the WE and cover some of the Ag atoms. This is evident in the spectra by the reduction in height of the Ag peak, as the peak height is directly related to the surface coverage of a species. [35] The spectrum obtained using $^{20}Ne^{+}$ (Figure S3) reveals the presence of adsorbed S and Mg on the surface, which is in line with the expectations from the electrolyte. No other changes to the surface were observed.

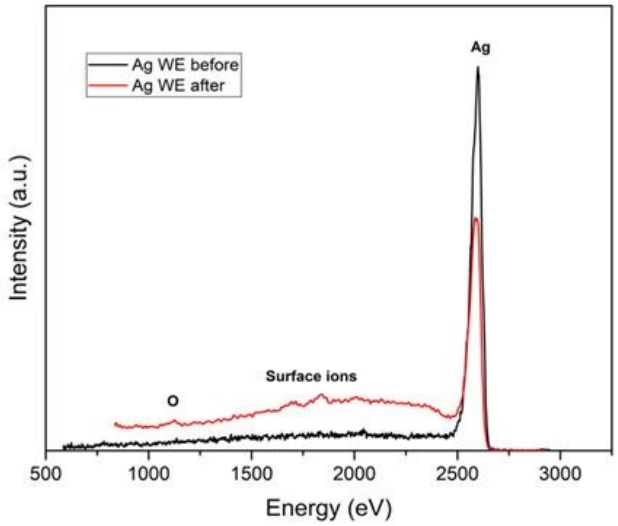

Figure 6 LEIS spectra of the Ag WE before (black curve) and after (red curve) the reaction in the H-cell. The reaction was performed in a 2.5 wt% gluconic acid solution with a $MgSO_4$ concentration of 1.5 wt%. The reaction time was 8 h. An Ag/AgCl (KCl saturated) RE and a platinum mesh CE were used. The spectra were measured under same conditions and parameters with $^{4}He^{+}$ 3keV.

A possible mechanism for the conversion of gluconic acid to glucose on silver as electrocatalytic material would be in line with our previous study of the electroreduction of xylonic acid on gold as electrocatalytic material. [24] The mechanism was determined via a combination of Reax FF molecular dynamic simulations and nudged elastic band simulation. [24] The carboxyl group of the gluconic acid would be being adsorbed on the silver surface. In addition, the sulfuric acid would be adsorbed on the silver electrode next to the gluconic acid. A hydrogen atom of the sulfuric acid would interact with the hydroxy part of the carboxyl group of the gluconic acid. The hydrogen is transferred to the gluconic acid molecule and water would be split. A second hydrogen atom would interact with the carbon of the previous gluconic acid molecule and glucose would be desorbed of the silver electrode.

Conclusions

In this investigation, we demonstrate a sustainable approach for the electrocatalytic reduction of gluconic acid into glucose as an SSL model component. The electrochemical conversion represents a safer and environment-neutral treatment compared to the conventional hydrothermal reduction. Within the framework of *Green Chemistry*, not only the conversion rate of an electrocatalytic material needs to be considered, but also the impact of the metal on the environment and the financial factor. In terms of ecological and economical aspects, silver proves to be a superior electrocatalyst compared to the previously reported gold working electrode. A potential screening of the reaction within the range of −0.66 V to −1.66 V *vs*. RHE revealed that the highest conversion rate was achieved at a potential of −1.56 V *vs*. RHE. Despite achieving low conversion rates throughout the entire potential range, the morphological and topographical analysis of the electrocatalyst using SEM, EDS, and XPS revealed no significant impact of the substances on the silver wire during the reaction. LEIS analysis indicated that the WE remained largely unaffected, except for the adsorption of ions from the electrolyte on the WE's surface and slight surface oxidation.

The electrocatalytic behaviour of silver resembles comparable trends as for the electrocatalytic CO_2RR and NRR, where a maximum conversion is reached at one cathodic potential before the HER is the dominant reaction at the electrode surface. Our work sheds light on the major challenge when considering the combination of electrocatalysis and the biorefinery concept toward the development of a sustainable side-stream valorization. Despite the low conversion rate toward glucose, this approach holds promise for the environmentally friendly and sustainable valorization of side-streams in the pulp and paper industry. Such *bioelectrofinery* would combine both electrocatalysis and the biorefinery concept, offering as such exciting opportunities for a circular economy empowered by renewable energy.

Conflicts of interest

There are no conflicts to declare.

View Article Online
DOI: 10.1039/D3CY00897E

Acknowledgements

We would like to acknowledge the Austrian government, the provinces of Lower Austria, Upper Austria, and Carinthia, as well as Lenzing AG, for financial support. We would like to acknowledge, Gesellschaft für Forschungsfoerderung NOE (FTI21-D002) and EFRE REACT-EU for the financial support. Also, we would like to express our gratitude to the Johannes Kepler University, Linz, the University of Natural Resources and Life Science (BOKU), Vienna, the University of Wuppertal and Lenzing AG for their in-kind contributions. Furthermore, we would like to thank the colleague from Wood K+ Markus Huemer, as well as Erwin Malzner, Walter Milacher and their teams for the support in the laboratories of Lenzing AG.

Notes and references

[1] F. W. S. Lucas, R. G. Grim, S. A. Tacey, C. A. Downes, J. Hasse, A. M. Roman, C. A. Farberow, J. A. Schaidle, A. Holewinski, *ACS Energy Lett.,* 2021, **6**, 1205–1270.

[2] United Nations Environment Programme, *Land Restoration for Achieving the Sustainable Development Goals. An International Resource Panel Think Piece*, United Nations, New York, 2020.

[3] M. Garedew, F. Lin, B. Song, T. M. DeWinter, J. E. Jackson, C. M. Saffron, C. H. Lam, P. T. Anastas, *ChemSusChem,* 2020, **13**, 4214–4237.

[4] N. Tripathi, C. D. Hills, R. S. Singh, C. J. Atkinson, *npj Clim Atmos Sci,* 2019, **2**, 35 (2019).

[5] a) T. Mai, D. Sandor, R. Wiser, T. Schneider, *Renewable Electricity Futures Study: Executive Summar*, 2012; b) A. J. Ragauskas et al., *N. Y. sci. j.* 2006, **311**, 484–489;

[6] S. R. Waldvogel, *Beilstein J. Org. Chem.* 2015, **11**, 949–950.

[7] MarketsandMarkets, *Biorefinery Market by Type (First Generation, Second Generation, and Third Generation), Technology (Industrial Biotechnology, Physico-Chemical, and Thermochemical), Product (Energy driven, and Material driven) and Region - Global Forecast to 2027*, **December /** 2022.

[8] Y. M. Bar-On, R. Phillips, R. Milo, *Proceedings of the National Academy of Sciences of the United States of America,* 2018, **115**, 6506–6511.

[9] a) K. Schlackl, R. H. Bischof, K. Fackler, W. Samhaber, *Sep. Purif. Technol.,* 2020, **250**, 117177; b) C. Rueda, P. A. Calvo, G. Moncalián, G. Ruiz, A. Coz, *J. Chem. Technol. Biotechnol.,* 2015, *90*, 2218–2226; c) Nigam J. M., *ACS Appl. Mater. Interfaces,* 2001, **26**, 145–150; d) D. Humpert, M. Ebrahimi, A. Stroh, P. Czermak, *Membr.* 2019, *9*,

[10] D. L. A. Fernandes, C. M. Silva, A. M. R. B. Xavier, D. V. Evtuguin, *J. Biotechnol.,* 2012, **162**, 415–421.

[11] D. Cannella, C. C. Hsieh, C. Felby, H. Jorgensen, *Biotechnol. Biofuels* 2012, **5**, 1–10.

[12] a) S. K. Bhatia, S. S. Jagtap, A. A. Bedekar, R. K. Bhatia, A. K. Patel, D. Pant, J. Rajesh Banu, C. V. Rao, Y.-G. Kim, Y.-H. Yang, *Bioresour. Technol.,* 2020, **300**, 122724; b) J. Fernández-Rodríguez, A. García, A. Coz, J. Labidi, *Sep. Purif. Technol.* 2015, **152**, 172–179;

[13] Grand View Research, *Glucose Market Size, Share & Trends Analysis Report By Form (Syrup, Solid), By Application (F&B, Pharmaceutical, Cosmetic & Personal Care, Pulp & Paper), By Region, And Segment Forecasts, 2020 - 2028,* GVR-4-68039-494-2 ed., 2019.

[14] B. García, A. Orozco-Saumell, M. López Granados, J. Moreno, J. Iglesias, *ACS Sustainable Chem. Eng.,* 2021, **9**, 14857–14867.

[15] Glattfeld J. W. E., Shaver E. H., *J. Am. Chem. Soc.,* 1927, **49**, 2305–2308.

[16] Marino D., Stöckmann D., Kriescher S., Stiefel S., Wessling M., *Green Chem.,* 2016, **18**, 6021–6028.

[17] J. R. Rostrup-Nielsen in *Progress in Catalyst Deactivation* (Ed.: J. L. Figueiredo), Springer Netherlands, Dordrecht, 1982.

[18] B. Hoffer, E. Crezee, F. Devred, P. Mooijman, W. Sloof, P. Kooyman, A. van Langeveld, F. Kapteijn, J. Moulijn, *Appl. Catal. A-GEN,* 2003, **253**, 437–452.

[19] a) S. R. Pereira, D. J. Portugal-Nunes, D. V. Evtuguin, L. S. Serafim, A. M. Xavier, *Process Biochem.,* 2013, **48**, 272–282; b) David W Goheen, 35253044;

[20] W.-J. Liu et al., *Nat. Commun.,* 2020, **11**, 265.

[21] A. T. Governo, L. Proença, P. Parpot, M. Lopes, I. Fonseca, *Electrochim. Acta,* 2004, **49**, 1535–1545.

[22] Y. Cao, T. Noël, *Org Process Res Dev* 2019, **23**, 403–408.

[23] P. Parpot, A. Bettencourt, G. Chamoulaud, K. Kokoh, E. Belgsir, *Electrochim. Acta,* 2004, **49**, 397–403.

[24] M. Wolfsgruber, B. V. M. Rodrigues, M. G. Da Cruz, R. H. Bischof, S. Budnyk, B. Beele, S. Monti, G. Barcaro, C. Paulik, A. Slabon, *ACS Sustain. Chem. Eng.,* 2023, **11**, 312–321.

[25] Galmarley Ltd T/A BullionVault, "Gold price chart", to be found under https://www.bullionvault.com/gold-price-chart.do, 2023.

[26] Galmarley Ltd T/A BullionVault, "Silver price chart", to be found under https://www.bullionvault.com/silver-price-chart.do, 2023.

[27] P. Nuss, M. J. Eckelman, *PLOS ONE,* 2014, *9*, e101298.

[28] a) B. A. Rosen, A. Salehi-Khojin, M. R. Thorson, W. Zhu, D. T. Whipple, P. J. A. Kenis, R. I. Masel, *Science (New York, N.Y.),* 2011, **334**, 643–644; b) T. Hatsukade, K. P. Kuhl, E.

View Article Online
DOI: 10.1039/D3CY00897E

R. Cave, D. N. Abram, T. F. Jaramillo, *Phys. Chem. Chem. Phys.,* 2014, **16**, 13814–13819;

[29] I. Moussallem, S. Pinnow, N. Wagner, T. Turek, *Chem. Eng. Process.,* 2012, **52**, 125–131.

[30] H. Liu, T.-H. Lee, Y. Chen, E. W. Cochran, W. Li, *Green Chem.,* 2021, **23**, 5056–5063.

[31] a) J. Feng, S. Zeng, J. Feng, H. Dong, X. P. Zhang, *Chin. J. Chem.,* 2018, **36**; b) G. Marcandalli, M. C. O. Monteiro, A. Goyal, M. T. M. Koper, *Accounts of Chemical Research,* 2022, *55*, 1900–1911;

[32] Hereus Holding, "Hereus Edelmetallpreise - Aktuell", to be found under https://www.heraeus.com/de/hpm/market_reports/prices/current_hu.html, 2023.

[33] "Mineralienatlas - Fossilienatlas. Silber", to be found under https://www.heraeus.com/de/hpm/market_reports/prices/current_hu.html.

[34] Y. Chen, M. W. Kanan, *J. Am. Chem. Soc.,* 2012, *134*, 1986–1989.

[35] H. ter Veen, T. Kim, I. E. Wachs, H. H. Brongersma, *Catal. Today,* 2009, **140**, 197–201.